Field-emission based vacuum device for the generation of terahertz waves

Ming-Chieh Lin,[a] Kuo-Hua Huang, Pu-Shih Lu, Pei-Yi Lin, and Ruei-Fu Jao
NanoScience Simulation Laboratory, Department of Physics, Fu Jen University, Taiwan, Republic of China

(Received 30 September 2004; accepted 3 January 2005; published 7 April 2005)

Terahertz (THz), waves i.e., electromagnetic radiation in the frequency extending from 0.1 to 10 THz (wavelengths of 3 mm down to 0.03 mm), have been used to characterize the electronic, vibrational, and compositional properties of solid, liquid, and gas phase materials during the past decade. More and more applications in imaging science and technology call for the well development of THz wave sources. Amplification and generation of a high frequency electromagnetic wave are a common interest of field emission based devices. In the present work, we propose a vacuum electronic device based on field emission mechanism for the generation of THz waves. To verify our thinking and designs, the cold tests and the hot tests have been studied via the simulation tools, SUPERFISH and MAGIC. In the hot tests, two types of electron emission mechanisms are considered. One is the field emission and the other is the explosive emission. The preliminary design of the device is carried out and tested by the numerical simulations. The simulation results show that an electronic efficiency up to 4% can be achieved without employing any magnetic circuits. © *2005 American Vacuum Society.* [DOI: 10.1116/1.1864063]

I. INTRODUCTION

Many rotational and vibrational spectra of various liquid and gas molecules lie within the terahertz (THz) frequency band, and their unique resonance lines in the THz wave spectrum allow us to identify their molecular structures. More and more applications in imaging science and technology call for the well development of THz wave sources. There are mainly two methods for the generation of electromagnetic (EM) waves. One is a quantum mechanical method, which deals with the use of the conduction electrons in a solid, i.e., laser, suitable for optical radiation. The other is a classical process, which deals with the use of streaming electrons in a vacuum, i.e., maser, suitable for microwave generation. The opposing limitations of the two processes result in the long-recognized millimeter and submillimeter gap in the electromagnetic spectrum where the achievable power falls to low levels from both the long- and short-wavelength regions. The well-known electron cyclotron masers (ECM) provide the solution.[1] In the past four decades, the ECM has undergone a remarkably successful evolution from basic research to device implementation, almost filling the gap. However, degradation of power generation in THz band is still present.

Amplification and generation of a high frequency electromagnetic wave are a common interest of field emission array (FEA) based devices.[2] In the present work, we propose a vacuum electronic device based on field emission mechanism for the generation of THz waves. It is well known that a transition radiation is emitted when an electron passes through an ideally conducting screen in vacuum[3] and a diffraction radiation is emitted when an electron of a constant velocity passes by a metallic structure.[4,5] The field-emission electrons directly pass through the cathode-anode gap, bunching and synchronizing with the THz wave through the well-tailored metallic structures, i.e., the oscillating electric field in the y direction coupled through in the x direction. Simulation tools such as SUPERFISH[6] and MAGIC[7] are used to verify our thinking and designs.

II. CIRCUIT MODEL AND SIMULATION TOOLS

Two types of interacting structures are considered. One is double-sided coupled cavity and the other is single-sided coupled cavity. The former is suitable for linear beam interactions and the latter is suitable for cross-field interactions. These slow wave structures can be easily fabricated via today's technologies such as microelectromechanical systems (MEMS).

A. Cold tests

The interacting structures are designed via numerical simulations in the frequency domain, i.e., cold tests. A two-dimensional (2D) finite-element-method based code SUPERFISH (developed by Los Alamos National Laboratory, NM) is used to acquire the preliminary geometry. Both the electric field patterns and the dispersion relations of the double-sided circuit model and the single-sided circuit model are obtained and investigated. As considering from conventional microwave theory, the final decision goes to the single-sided coupled cavity tailored for cross-field interactions, similar to a planar magnetron. Figure 1 shows the schematic of the field emission based THz wave generator we proposed. The anode consists of six coupled cavities and the cathode is some kind of field emission array (FEA). The areas marked "*I*" stand for insulators. A 2D finite-difference time-domain (FDTD) particle-in-cell (PIC) code MAGIC (developed by

[a]Also with the Institute of Nanotechnology at National Chiao Tung University in Taiwan as an adjunct assistant professor; present address: 510 Chung Cheng Rd, Hsinchuang, Taipei Hsien, Taiwan 24205, R. O. C.; electronic mail: mclin@mails.fju.edu.tw

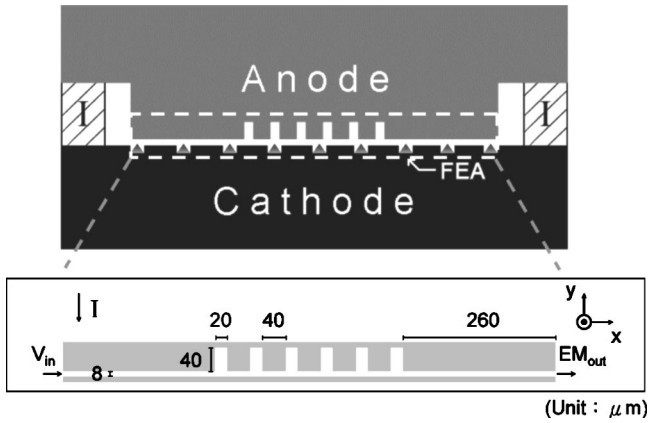

FIG. 1. Schematic of the field emission based THz generator with the cathode and anode indicated in the figure. Here, FEA stands for "field emission array," and area "*I*" is the insulator. The corresponding MAGIC simulation model is also shown.

MRC Co., VA) is also employed not only for verifying the designs but also for the convergence tests before jumping into time-consuming hot tests of the generation of THz waves. The 2D MAGIC model for the design also shown in Fig. 1 has been constructed for both the cold and hot tests. As inspired by the field patterns as shown in Fig. 2, i.e., π modes, no magnetic circuit is employed in our design. Detail geometry dimensions and boundary conditions are indicated, too. The material of the cavity is assumed to be a perfect conductor.

B. Hot tests

MAGIC is an electromagnetic particle-in-cell (EM PIC) code, based on the FDTD method for simulating plasma physics processes such as the processes that involve interactions between space charge and electromagnetic fields. Beginning from a specified initial state, the code simulates a physical process as it evolves in time. The full set of time-dependent Maxwell's equations is solved to obtain electromagnetic fields. Then, the complete Lorentz force equation is solved to obtain relativistic particle trajectories, and the continuity equation is solved to provide current and charge densities for Maxwell's equations. This self-consistent approach is commonly referred to as the EM PIC method, and is suitable for dealing with the interaction between charged particles and electromagnetic fields. The interaction between the charged particles is also included. In addition, the code has been provided with powerful algorithms to represent structural geometries, material properties, incoming and outgoing waves, particle emission processes, and so forth. As a result, 2D MAGIC is employed to do the hot tests of the field emission based THz wave generator. In the hot tests, two types of electron emission mechanisms are considered. One is the field emission and the other is the explosive emission.[8]

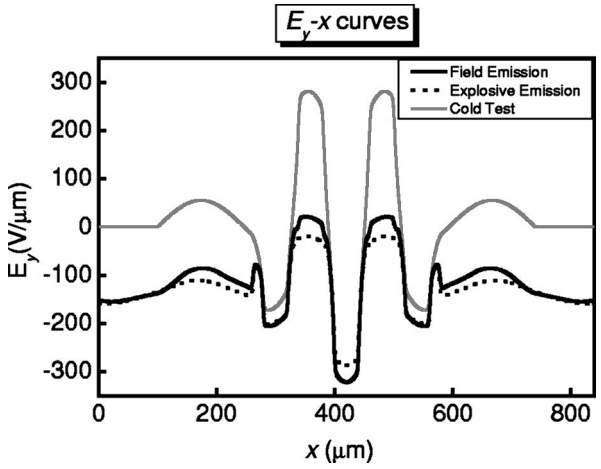

FIG. 2. $E_y - x$ curves of the cold test and the hot tests for two kinds of emission mechanisms, the field emission, and explosive emission, respectively.

C. Field emission

The field emission process is described by the Fowler–Nordheim equation[9–17]

$$J = \frac{AE_s^2}{\phi t(y)^2}\exp\left(\frac{-Bv(y)\phi^{3/2}}{E_s}\right), \tag{1}$$

where A and B are the Fowler–Nordheim constants, and ϕ is the effective work function assumed to be a constant allowed dependence on material and surface roughness.[17–19] One should note that the "effective work function" here is different from the work function as usually defined. The effective work function can be affected by the local electric fields, i.e, the Schottky effect.[18,19] The normal electric field at the cathode surface E_s is computed from the application of Gauss's law to the half-cell immediately above the emitting surface, or

$$E_s = (E_c A_c - q/\varepsilon_0)/A_s, \tag{2}$$

where E_c is the electric field at the half-grid, A_c and A_s are the cell areas at half-grid and surface, respectively, and q is the existing charge in the half-cell. The functions $t(y)$ and $v(y)$ were introduced by Spindt *et al.*,[20] and approximated by

$$t(y)^2 = 1.1, \tag{3}$$

$$v(y) = 0.95 - y^2, \tag{4}$$

$$y = 3.79 \times 10^{-5}\, E_s^{1/2}/\phi, \tag{5}$$

where y is the Schottky lowering of the effective work function barrier.

D. Explosive emission

Explosive emission results from plasma formation on a material surface. Almost any surface exhibits microscopic protrusions, or "whiskers." When exposed to high voltages, electric field enhancement at the whiskers can cause significant field emission. Subsequently, the whisker may get erosion due to Joule heating, resulting in the formation of plasma on the material surface. This surface plasma will

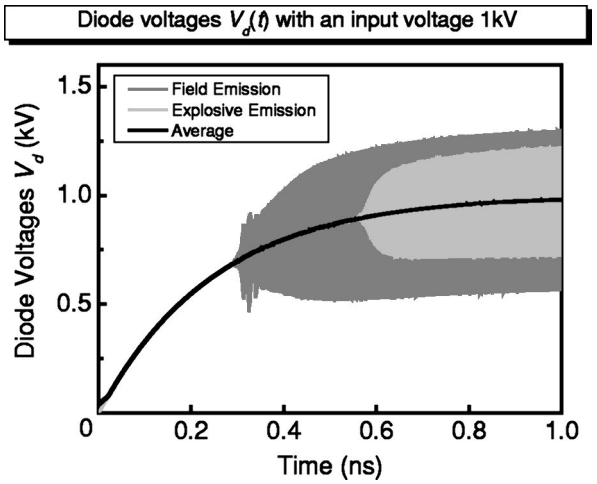

FIG. 3. Monitored diode voltage $V_d(t)$ curves with an input voltage 1 kV.

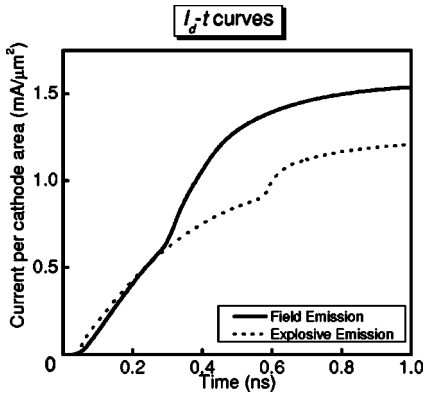

FIG. 5. Monitored $I_d(t)$ curves. I_d stands for the total current divided by the cathode area.

typically "emit" under the influence of the ambient electric field, with the species extracted from the plasma being determined by the sign of the field.[21,22] MAGIC largely ignores the physical details of the plasma formation process, relying instead on a phenomenological description. However, the particle emission itself is based upon Child's law of physics, specifically, the normal electric field vanishing at the plasma surface. In the phenomenological treatment of plasma formation, breakdown can occur only if the normally directed field at the half-cell E_c exceeds some specified breakdown field threshold, or $|E_c| > E_{\text{threshold}}$. This test is performed continuously for every surface cell on the emitting object. If the field at a particular cell exceeds the threshold, then that cell is said to "break down." A single, nonemitting cell between two emitting cells is also allowed to break down, even if the threshold is not exceeded. The time of breakdown is recorded for each cell that breaks down. Subsequently, every cell has its own history and is treated independently.

III. SIMULATION RESULTS AND DISCUSSION

The simulation results of the cold tests of the MAGIC code are consistent with that of the SUPERFISH code, although we did not show the comparisons. Figure 2 shows our calculated $E_y - x$ curves of the cold test and the hot tests for two kinds of emission mechanisms, the field emission and explosive emission, respectively. The discrepancy between the cold test and the hot tests is due to the applied diode voltages, i.e., voltages between the anode and the cathode, for the latter cases. In the hot tests, an input voltage $V_{\text{in}}(t) = V_{\max}[1 - \text{Exp}(-t/T_{\text{rise}})]$, where $V_{\max}$ is 1 kV and T_{rise} is 0.25 ns, is superposed on the structure between the anode and the cathode. For the field emission case, the effective work function is set as $\phi = 0.2$ eV which might be due to the high applied electric fields and the local field enhancements.[17–19] The threshold field is set to 23 V/μm for the explosive case, which is the default setting in the MAGIC code.[23] As one can see from Fig. 2, the resonance is operated on the correct mode, i.e., π mode. The resonant electric field for the field emission case is a little higher than that for the explosive emission. Our monitored time evolution of diode voltages for the two cases, the field emission and the explosive emission, respectively, is shown in Fig. 3. The diode voltage corresponding to the field emission starts oscillating earlier than that corresponding to the explosive emission. The average of the data is also shown in the figure. The fast Fourier transformation (FFT) of the voltage curves is shown in Fig. 4. The resonant frequency of the field emission case is about 1.055 THz and that of the explosive emission case is 1.076

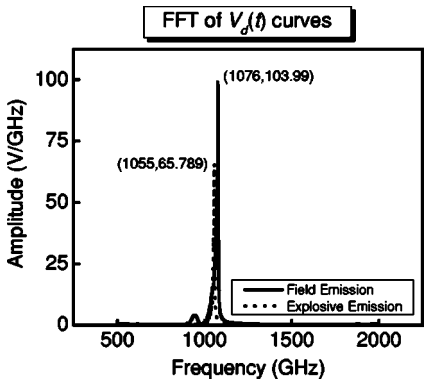

FIG. 4. Fast Fourier transform (FFT) of the diode voltage $V_d(t)$ curves.

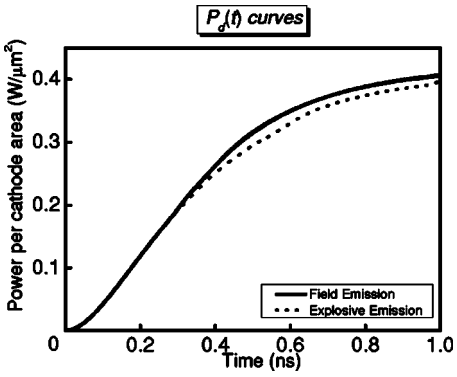

FIG. 6. Monitored $P_d(t)$ curves. P_d stands for the output power divided by the cathode area.

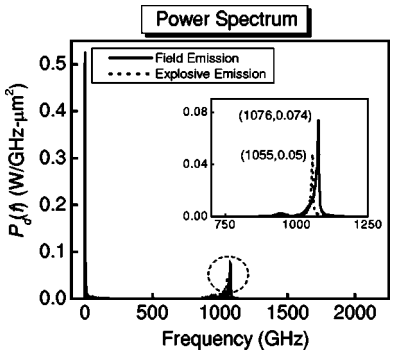

FIG. 7. Radiation power spectrum $P_d(f)$ for field emission and explosive emission modes.

THz. The amplitude of the former case is larger than that of the latter case. Figure 5 shows our monitored average diode current per cathode area for the two cases. Due to the low effective work function we assumed for the FEA, the field emission current from the cathode would be higher than the space-charge limiting current of the interaction structure. The average current of the field emission is larger than that of the explosive emission.

The output power of the device is also monitored. Figure 6 shows our monitored average power per cathode area for the two cases. The output power includes low frequency electromagnetic waves as well. It is difficult to separate the component of THz waves from the monitored output power in the time domain, so that the results of the two cases are similar. However, it is easy to analyze the THz waves generated by the field emission based devices with the EM power spectrum, as shown in Fig. 7. The output power of the THz wave for the field emission case is about 0.074 $W/\mu m^2$ and that for the explosive emission case is 0.05 $W/\mu m^2$. The estimated values of the corresponding beam power are about 1.53 and 1.29 $W/\mu m^2$, respectively. The electronic efficiency of the device, i.e., the output power divided by the beam power, can be easily estimated to be up to 4%. Further investigation is continuing. Detail interaction mechanisms are under study to improve the efficiency.

IV. CONCLUSION

We propose a vacuum electronic device based on the field emission mechanism for the generation of THz waves. The preliminary design of the device is carried out and tested by the numerical simulations. To verify our thinking and designs, the cold tests and the hot tests have been done using the simulation tools, SUPERFISH and MAGIC. The simulation results show that an electronic efficiency up to 4% can be achieved with no external magnetic fields. The field emission based vacuum device seems to be a good candidate for the generation of THz waves. Further investigations are underway to realize the detail interaction mechanisms and to confirm the design before fabrication of real circuits.

ACKNOWLEDGMENTS

This work was partially supported by the National Science Council, Taiwan, R. O. C., under Grant No. NSC 93-2112-M-030-007 and the National Center for High-performance Computing, Taiwan, R. O. C. which provides the MAGIC code and the computing resources.

[1]K. R. Chu, Rev. Mod. Phys. **76**, 1 (2004).
[2]K. Yokoo and T. Ishihara, *Conference Digest of IVMC'95*, Oregon, 1995, p. 123.
[3]F. G. Bass and V. M. Yakovenko, Usp. Fiz. Nauk **86**, 189 (1965) [Sov. Phys. Usp. **8**, 420 (1965)].
[4]B. M. Bolotovskii and G. M. Voskresenskii, Usp. Fiz. Nauk **88**, 209 (1966) [Sov. Phys. Usp. **9**, 73 (1966)].
[5]P. M. Van den Berg and A. J. A. Nicia, J. Phys. A **9**, 1133 (1976).
[6]J. H. Billen and L. M. Young, *Poisson Superfish*, LA-UR-96-1834 (Los Alamos National Laboratory, NM, 2003).
[7]B. Goplen, L. Ludeking, D. Smithe, and G. Warren, Comput. Phys. Commun. **87**, 54 (1995).
[8]R. B. Miller, *An Introduction to the Physics of Intense Charged Particle Beams* (Plenum, New York, 1982).
[9]R. H. Fowler and L. W. Nordheim, Proc. R. Soc. London, Ser. A **119**, 173 (1929).
[10]L. W. Nordheim, Proc. R. Soc. London, Ser. A **121**, 626 (1928).
[11]L. W. Nordheim, Z. Phys. **30**, 177 (1929).
[12]W. Schottky, Z. Phys. **14**, 63 (1923).
[13]N. H. Frank and L. A. Young, Phys. Rev. **38**, 80 (1931).
[14]E. Guth and C. J. Mullin, Phys. Rev. **61**, 339 (1942).
[15]D. V. Gogate and D. S. Kothari, Phys. Rev. **61**, 349 (1942).
[16]S. Gasiorowicz, *Quantum Physics*, 2nd ed. (Wiley, New York, 1996).
[17]M. C. Lin and D. S. Chuu, Appl. Phys. Lett. **80**, 4262 (2002).
[18]C. Kim and B. Kim, Phys. Rev. B **65**, 165418 (2002).
[19]J. A. Nation *et al.*, Proc. IEEE **87**, 865 (1999).
[20]C. A. Spindt, I. Brodie, L. Humphrey, and E. R. Westerberg, J. Appl. Phys. **47**, 5248 (1976).
[21]S. A. Goldstein and R. Lee, Phys. Rev. Lett. **35**, 1079 (1975).
[22]E. H. Choi, H. M. Shin, and D. I. Choi, J. Appl. Phys. **61**, 2160 (1987).
[23]B. Goplen, L. Ludeking, D. Smithe, and G. Warren, *MAGIC User's Manual* (Mission Research Corp., VA, 1997) MRC/WDC-R-409.